Effect of Delamination on Natural Frequencies of E-glass and S-glass Epoxy Composite Plates

P. K. Karsh[1,2,*], Bindi Thakkar[1], R. R. Kumar[2,3], Abhijeet Kumar[2] and Sudip Dey[2]

[1]*Department of Mechanical Engineering, Parul Institute of Engineering & Technology, Parul University, Vadodara, India*
[2]*Department of Mechanical Engineering, National Institute of Technology Silchar, India*
[3]*School of Engineering, Jawaharlal Nehru University, New Delhi, India*
E-mail: pradeepkarsh@gmail.com
[*]*Corresponding Author*

Received 18 December 2020; Accepted 19 March 2021;
Publication 19 May 2021

Abstract

The delamination is one of the major modes of failure occurring in the laminated composite due to insufficient bonding between the layers. In this paper, the natural frequencies of delaminated S-glass and E-glass epoxy cantilever composite plates are presented by employing the finite element method (FEM) approach. The rotary inertia and transverse shear deformation are considered in the present study. The effect of parameters such as the location of delamination along the length, across the thickness, the percentage of delamination, and ply-orientation angle on first three natural frequencies of the cantilever plates are presented for S-glass and E-glass epoxy composites. The standard eigenvalue problem is solved to obtain the natural frequencies and corresponding mode shapes. First three mode shape of S-Glass and E-Glass epoxy laminated composites are portrayed corresponding to different ply angle of lamina.

European Journal of Computational Mechanics, Vol. 29_4–6, 437–458.
doi: 10.13052/ejcm1779-7179.29466

Keywords: Natural frequency, S-glass epoxy, E-glass epoxy, delamination, finite element method.

1 Introduction

Today scientists and researchers are working on designing and manufacturing of lightweight and stiffer materials such as laminated composites. Laminated composite plates have an extensive technological application in many areas such as aircraft, marine, automobiles and other applications where weight sensitiveness is of prime importance because of its outrageous specific stiffness and favourable specific strength. Although composites are very useful, where lightweight and flexible structures are required but they failed at the higher temperature and cyclic load due to delamination. The strength and stiffness of the structures are mostly checked by delamination in case of laminated composites leading to the structural instability. The delamination of layers occurs due to insufficient bonding and residual stresses between the layers. The delamination may occur due to manufacturing defects, externally applied repeated impact load, and irregularities in surfaces. The natural frequencies are decreased by reducing the stiffness (greatly affected by the delamination) of the plate. Therefore, it is required to analyze the dynamic characteristics of composite plates under delamination to ensure operational safety.

In past, many researchers conducted research on natural frequency analysis of delaminated composite plates such as [1] presented review on delaminated plates and beam and examined the elements influencing the vibration of the delaminated composites. Nanda and Sahu applied different shell theories to determine the vibration responses of composite shells in the absence of damping with or without delamination by using the FE method [2]. Campanelli and Engblom formulated a finite element-based model to contemplate the influence of delamination on the dynamic behaviours of composite plates [3]. A 3D FEM based methodology is developed by F. Fu [4] to investigate the behaviour of tall building subjected to fire. Hu et al. [5] employed higher-order plate theory to analyse vibrational attributes of composite plates with delamination. FEM based algorithm is developed by Polatov et al. [6] for getting the solution for elastoplastic deformation of composites. Krawczuk and Ostachowicz [7] developed a model to evaluate the free vibration of a cantilever beam of composite material with a crack in the transverse direction. Kaya et al. [8] evaluated the impact of the surrounding condition for first three natural frequencies of carbon fibre reinforced composites by using

experimental method and results are further validated with ANSYS results. Dey et al. [9] carried out a stochastic investigation of natural frequencies of cantilever composite plate by incorporating an artificial neural network (ANN) and portrayed the influence of stochasticity in properties of the material. Byrd and Birman [10] explored the impact of matrix cracks on mechanical behaviour and frequencies due to vibration for cross-ply composite beams. Ramkumar et al. [11] applied eigenvalue boundary problems to investigate the vital characteristics of composite beams due to delamination. Wang et al. [12] presented a general solution for a beam having a split and non-split region. Kalita et al. [13] determined the natural frequency response of laminated plates by employing FEM and determined the influence of ply orientation angle, the ratio of length to thickness and number of plies. Ercopur and Kiral [14] used ANSYS for evaluating the natural frequency of composite plates due to delamination under different boundary conditions. Saravanos and Hopkins [15] employed an analytical approach in light of classical laminated plate theory to explore the impact of delamination on vibration characteristics. Kisa [16] utilized FEM and component modal synthesis techniques for free vibration investigation of a cantilever beam of composite with several cracks considering the effect of damping and delamination. Perel [17] employed FEM to analyse the dynamic characteristics of the composite beam. Tornabene and Viola [18] investigated in-plane fundamental natural frequencies for thin as well as thick non-uniform roundabout curves in unharmed and harmed setups with different end conditions. Qatu and Leissa [19] performed extensive work on pre-twisted composite plates wherein the Ritz method and shell theory is utilized to define the vibrational characteristics of stationary plates. Some researchers applied the deterministic and stochastic approach for the free vibration behaviour analysis of composite and FGM structures [20–23].

The novelty of the present paper includes determination of effect of delamination on the first three natural frequencies of the S-glass and E-glass cantilever composite plate and compared the results of these two composites. Also, the effects of the number of delamination, location of delamination, percentage of delamination as well as plate geometry on the first three natural frequencies are determined. A comparative study of the natural frequencies of two different types of composites such as E-glass epoxy and S-glass epoxy has carried out. A finite element approach has applied for the deterministic natural frequency analysis, in which plate is discretised into 64 elements. The first three mode shapes plate for both E-glass and S-glass composite are also determined by using the ANSYS software.

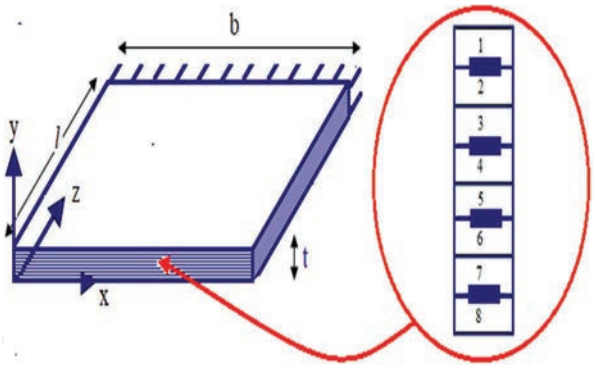

Figure 1 Laminated composite cantilever plate through multiple delaminations.

2 Mathematical Formulation

The dynamic equilibrium equation in the absence of external load and damping [24] can be written as

$$[M]\{\ddot{\delta}\} + [K]\{\delta\} = 0 \tag{1}$$

where, $[M]$ implies global mass matrix, $[K]$ implies stiffness matrix and $\{\delta\}$ is a displacement vector. The stresses at any point can be expressed as [25]

$$\begin{bmatrix} \sigma_{xx} \\ \sigma_{yy} \\ \tau_{xy} \\ \tau_{xz} \\ \tau_{yz} \end{bmatrix} = \begin{bmatrix} q_{11} & q_{12} & q_{16} & 0 & 0 \\ q_{12} & q_{22} & q_{26} & 0 & 0 \\ q_{16} & q_{26} & q_{66} & 0 & 0 \\ 0 & 0 & 0 & q_{44} & q_{45} \\ 0 & 0 & 0 & q_{45} & q_{55} \end{bmatrix} \begin{bmatrix} \varepsilon_{xx} \\ \varepsilon_{yy} \\ \gamma'_{xy} \\ \gamma'_{xz} \\ \gamma'_{yz} \end{bmatrix} \tag{2}$$

where, $[q_{ij}]$ is the elastic constant matrix. For laminated composite, elasticity matrix is given by

$$[D''] = \begin{bmatrix} E^c_{lm} & E^b_{lm} & 0 \\ E^b_{lm} & D_{lm} & 0 \\ 0 & 0 & S_{lm} \end{bmatrix} \tag{3}$$

where,

$$[E^c_{lm}, E^b_{lm}, D_{lm}] = \sum_{k=1}^{n} \int_{z_{k-1}}^{z_k} [q_{lm}][1, z, z^2]dz \quad l, m = 1, 2 \text{ and } 6 \tag{4}$$

$$U_1 = \frac{1}{2} \int_{VOL} \{\bar{\delta}_e\}^T [H][D''][H]\{\bar{\delta}_e\} d\phi \tag{5}$$

$$\text{i.e., } U_1 = \frac{1}{2}\{\bar{\delta}_e\}^T[K'_e]\{\bar{\delta}_e\} \tag{6}$$

$$[S_{lm}] = \sum \int_{z_{k-1}}^{z_k} \beta[q_{i_{lm}}]_k dz \quad l, m = 4, 5 \tag{7}$$

where $\{\delta_e\}$ represents nodal displacement vector of the element, $[H]$ represents strain-displacement matrix, $[D'']$ is the elasticity matrix and β is the shear correction factor assumed as 0.833.

2.1 Multipoint Constraints

The cross-sectional view of the delaminated composite crack tip of a plate is depicted in Figure 2. The nodes of all the three plate elements are arranged in order to form the common node *A*. Plate element 1 having thickness 'h' shows an un-delaminated area whereas there is the region of delamination at the boundary of plate element 2 and 3 of thickness 'h_2' and 'h_3'. The nodal displacement (u_i, v_i, w_i) of second and third element for crack tip can be formulated as [26]

$$\begin{aligned} u_i &= \hat{u}_i - (z - \hat{z}_i)\theta^{\circ}_{xi} \\ v_i &= \hat{v}_i - (z - \hat{z}_i)\theta^{\circ}_{yi} \\ w_i &= \hat{w}_i \quad (\text{where, } i = 2 \text{ and } 3) \end{aligned} \tag{8}$$

where, midplane displacements are represented as $\hat{u}_i, \hat{v}_i, \hat{w}_i$ and at mid-plane the co-ordinate of i element in the z-direction is $\hat{z}_i$. The above-mentioned equations hold good for element 1 as well and $\hat{z}_1$ become equal to 0.

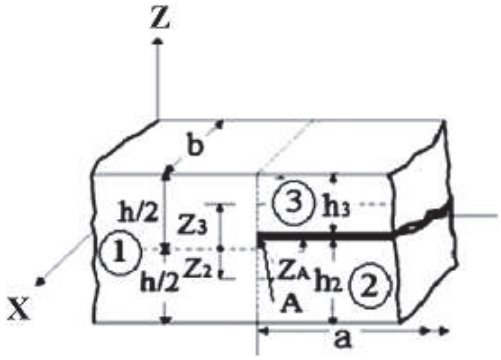

Figure 2 Delamination crack at the tip of plate elements.

Consider θ_x, θ_y as rotation componets about x and y-axis. At common node the transverse displacements and rotations can be expressed as

$$\begin{aligned} w_1 &= w_2 = w_3 = w \\ \theta_{x1} &= \theta_{x2} = \theta_{x3} = \theta_x \\ \theta_{y1} &= \theta_{y2} = \theta_{y3} = \theta_y \end{aligned} \tag{9}$$

All three elements have equal in-plane displacements at the crack tip and represented as

$$\begin{aligned} \hat{u}_2 &= \hat{u}_1 - \hat{z}_2\theta_x \\ \hat{v}_2 &= \hat{v}_1 - \hat{z}_2\theta_y \\ \hat{u}_3 &= \hat{u}_1 - \hat{z}_3\theta_x \\ \hat{v}_3 &= \hat{v}_1 - \hat{z}_3\theta_y \end{aligned} \tag{10}$$

where $\hat{u}_1$ implies displacement at the mid-plane for first element. The relation between rotation of elements and displacements at the delamination crack tip is provided in Equations (9) and (10). These equations satisfy the compatibility equations of displacement and rotations and these equations are employed for the finite element formulation in the present study. The strain between second and third elements at mid-plane are expressed by Equation (11).

$$\{\varepsilon^\circ\}_j = \{\varepsilon^\circ\}_1 + \hat{z}_j\{k\} \tag{11}$$

where $\{\varepsilon^\circ\}$ represents the strain vector at mid-plane, while $\{k\}$ is the curvature vector. For elements 1, 2 and 3 curvature vector have same value at the crack tip. This equation is the special case for element 1 when z'1 is equal to zero. For the element, 2 and 3 the in-plane moment resultants $\{M\}$ and stress- resultants $\{N\}$ expressed by,

$$\{N\}_m = [E^c]_m\{\varepsilon^\circ\}_1 + (\bar{z}_j[E^c]_m + [E^b]_m)\{K\} \tag{12}$$

$$\{M\}_m = [E^b]_m\{\varepsilon^\circ\}_1 + (\bar{z}_m[E^b]_m + [D]_m)\{k\} \tag{13}$$

Where the coefficients $[E^c]$ implies extension, $[E_b]$ implies bending-extension coupling and [*D*] implies bending stiffness for the laminated plate. The modified matrix of elasticity for the *n*th sub-laminate can be expressed as

$$[D]_n = \begin{bmatrix} E^c_{lm} & z^\circ_n E^c_{lm} + E^b_{lm} & 0 \\ E^b_{lm} & z^\circ_n E^c_{lm} + D_{lm} & 0 \\ 0 & 0 & S_{lm} \end{bmatrix} \tag{14}$$

where,

$$[E^c_{lm}]_n = \int_{-t/2+z^o_n}^{t/2+z^o_n} [q]dz \tag{15}$$

$$[E^b_{lm}]_n = \int_{-t/2+z^o_n}^{t/2+z^o_n} [q](z - z^0_n)dz = \int_{-t/2+z^o_n}^{t/2+z^o_n} [q]zdz - z^0_n[E^c_{lm}]_n \tag{16}$$

$$\begin{aligned}[D_{lm}]_n &= \int_{-t/2+z^o_n}^{t/2+z^o_n} [q](z - z^0_n)^2dz \\ &= \int_{-t/2+z^o_n}^{t/2+z^o_n} [q]z^2dz - 2z^0_n \int_{-t/2+z^o_n}^{t/2+z^o_n} [q]zdz + (z^0_n)^2[E^c_{lm}]_n \\ &\quad \text{where } l, m = 1, 2\end{aligned} \tag{17}$$

$$[S_{lm}]_n = \int_{-t/2+z^o_n}^{t/2+z^o_n} [q]dz \quad \text{where } l, m = 4, 5 \tag{18}$$

where, $[q]$ is the transformed reduced stiffness as defined by Jones [19] while z^0_n is the z co-ordinate of mid-plane of tth sublaminate. Thus the formulation based on the multipoint constraint conditions leads to unsymmetric stiffness matrix. The resultant moments and forces for the elements 1, 2, and 3 satisfy the following conditions [25]:

$$\{R\} = \{R\}_1 = \{R\}_2 + \{R\}_3 \tag{19}$$

$$\{S\} = \{S\}_1 = \{S\}_2 + \{S\}_3 + Z'_2\{N\}_2 + Z'_3\{N\}_3 \tag{20}$$

$$\{T\} = \{T\}_1 = \{T\}_2 + \{T\}_3 \tag{21}$$

where $\{T\}$ represents shear resultants in the transverse direction. An isoparametric element of a quadrilateral shape having eight nodes and five (three translations and two rotations) degrees of freedom are utilized and shape functions (S_f) can be expressed as:

$$\sum_{i=1}^{8} S_f = 1, \quad \sum_{i=1}^{8} \frac{\partial S_f}{\partial \chi} = 0, \quad \sum_{i=1}^{8} \frac{\partial S_f}{\partial \upsilon} = 0 \tag{22}$$

$$\begin{aligned}S_f &= (1 + \chi\chi_i)(1 + \upsilon\upsilon_i)(\chi\chi_i + \upsilon\upsilon_i - 1)/4 \\ &\quad (\text{for } i = 1, 2, 3 \text{ and } 4)\end{aligned} \tag{23}$$

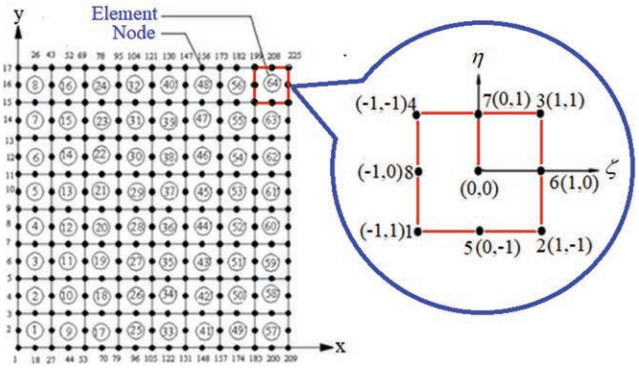

Figure 3 Finite element discretization of composite plate.

where, χ, υ represents the local natural coordinates of the element in which $\chi_i = +1$ for nodes 2, 3, 6, $\chi_i = -1$ for nodes 1, 4, 8, $\upsilon_i = +1$ for nodes 3, 4, 7, and $\upsilon_i = -1$ for nodes 1, 2, 5 as shown in Figure 3. The accuracy of the shape function is quantified by Equations (24) and (25)

$$S_f = (1-\chi^2)(1+\upsilon\upsilon_i)/2 \quad (\text{for } i = 5, 6) \tag{24}$$

$$S_f = (1-\upsilon^2)(1+\chi\chi_i)/2 \quad (\text{for } i = 6, 8) \tag{25}$$

For the eight-noded element at any point, the coordinates (x, y) can be derived from

$$x = \sum_{i=1}^{8} S_f x_i, \quad y = \sum_{i=1}^{8} S_f y_i \tag{26}$$

The relationship between the nodal degree of freedom and displacement at any point can be depicted as

$$u = \sum_{i=1}^{8} S_f u_i, \quad v = \sum_{i=1}^{8} S_f v_i, \quad w = \sum_{i=1}^{8} S_f w_i \tag{27}$$

$$\theta_x = \sum_{i=1}^{8} S_f \theta_{xi}, \quad \theta_y = \sum_{i=1}^{8} S_f \theta_{yi} \tag{28}$$

$$\begin{bmatrix} S_{f,x} \\ S_{f,y} \end{bmatrix} = [J]^{-1} \begin{bmatrix} S_{f,\zeta} \\ S_{f,\eta} \end{bmatrix} \tag{29}$$

where $[J] = \begin{bmatrix} x,\zeta & y,\zeta \\ x,\eta & y,\eta \end{bmatrix}$ is the Jacobian matrix.

3 Results and Discussion

In the current study, the effects of different input parameters on first three natural frequencies (Fundamental natural frequency (FNF), Second natural frequency (SNF), and Third natural frequency (TNF)) of composite cantilever plate are determined. The input parameters considered are as follows:

(a) Delamination along the length of the plate
(b) Delamination across the thickness of the plate
(c) Percentage of delamination
(d) Effect of the ply orientation angle of the plate

Figure 4 illustrates the flowchart for free vibration analysis employing the FE method in the composite plate. The plate is discretized into 64 number of elements with each element having five degrees of freedom (DOF). The finite element modeling is based on 8-layer square laminated glass-epoxy composite plates having width = length = 1 *m* and thickness = 4 *mm* with a configuration of bending stiff $[0°, 0°, \pm 30°]_S$, torsional stiff $[\pm 45°, \pm 45°]_S$ and quasi-isotropic $[0°, \pm 45°, 90°]_S$ until otherwise mentioned. The material properties of S-glass and E-glass composites are given in Table 1(a).

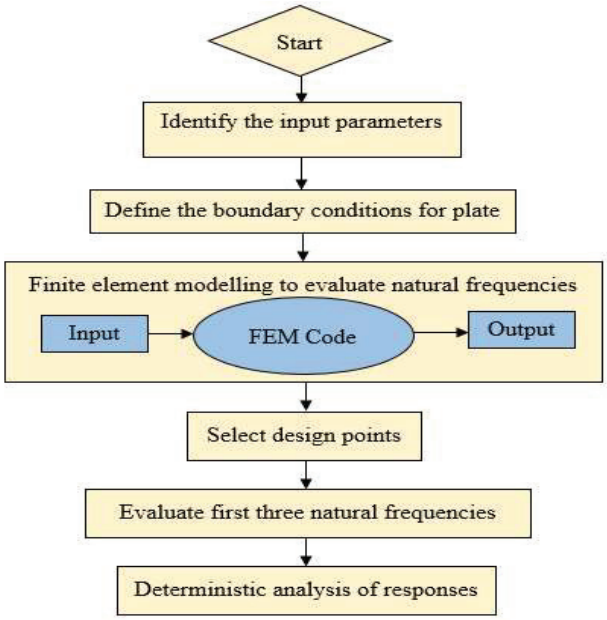

Figure 4 Flowchart of free vibration analysis using FEM.

Table 1(a) Material properties of glass-epoxy laminated plates

Material Properties	S-Glass	E-Glass
E_1	43 GPa	38.6 GPa
$E_2 = E_3$	8.9 GPa	8.27 GPa
$G_{12} = G_{13}$	4.5 GPa	4.14 GPa
G_{23}	1.8 GPa	1.656 GPa
$\upsilon_{12} = \upsilon_{13}$	0.27	0.26
$\upsilon_{21} = \upsilon_{31}$	0.006	0.006
$\upsilon_{23} = \upsilon_{32}$	0.40	0.26
ρ	2000 kg/m^3	2600 kg/m^3

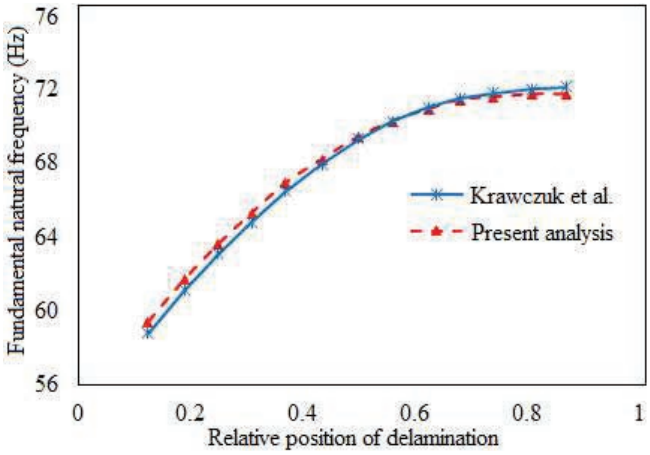

Figure 5 The relative effect of delamination with fundamental natural frequency for cantilever composite plate.

In the present study, FEM is incorporated to develop computer code. The evaluated results are compared and further validated with published literature's results [7] as shown in Figure 5. The present analysis depicts a very similar pattern as compared with the published literature results. It justifies the merit of developed codes and accuracy of the results. For more reliability of our results, one more validation is carried out for E-glass composite with material properties E1 = 72.7 GPa, E2 = E3 = 7.2 GPa, G12 = G13 = 3.76 GPa, G23 = 2.71 GPa, $\nu 12 = \nu 13 = 0.3$, $\nu 23 = 0.33$ and $\rho = 1566$ kg/m^3 as presented in Table 1(b).

Table 1(b) Validation of present results with the previously published results

Mode	Present FE Model	Ercopur and Kiral [28]
1	81.02	81.52
2	109.41	109.92
3	199.06	199.57

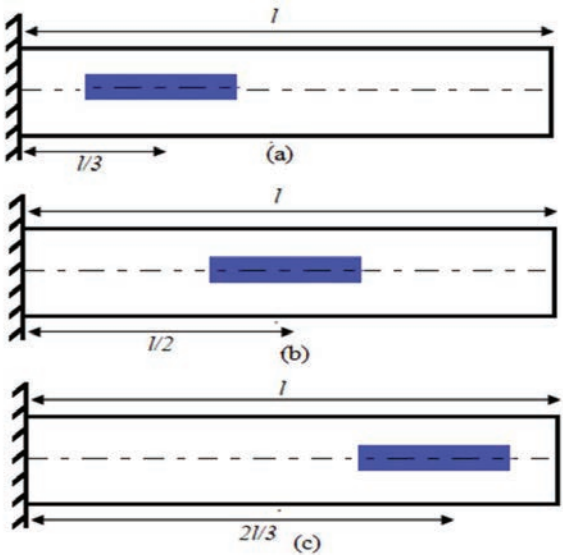

Figure 6 Various location of delamination throughout the length of the plate.

3.1 Analysis of Delamination Along the Length

The effects of delamination position laterally on the first three natural frequencies are discussed in this section. The presence of delamination causes loss of stiffness in the plate resulting in a decrement of natural frequencies of composite plates. The effects of delamination location on natural frequencies of *E*-glass and *S*-glass epoxy composites are given in Table 2, where '*a*' is the distance of delamination from the clamped end. The location of delamination along the length is presented in Figure 6. In this case, the percentage of delamination is considered as 25% of the length of the plate. The fundamental natural frequency decreases as moving away from the fixed end and lowest values are obtained near the free end for different configuration of the laminated composite plates. However, the natural frequencies of the S-Glass epoxy composites are greater than E-Glass epoxy composites, while

Table 2 Effects of delamination location along the length of the plate on the first three natural frequencies of *E*-glass and *S*-glass composite plates

Delamination Along with the Length	Fiber Orientation	Natural Frequencies (rad/s)					
		E-Glass			*S*-Glass		
		FNF	SNF	TNF	FNF	SNF	TNF
$a = l/3$	$[0^\circ, 0^\circ, \pm 30^\circ]$	4.503	23.625	78.801	5.364	28.104	93.826
	$[\pm 45^\circ, \pm 45^\circ]$	4.659	26.382	85.038	5.536	31.386	101.295
	$[0^\circ, \pm 45^\circ, \pm 90^\circ]$	5.048	27.721	88.573	6.010	33.022	105.661
$a = l/2$	$[0^\circ, 0^\circ, \pm 30^\circ]$	4.497	23.642	78.829	5.357	28.124	93.862
	$[\pm 45^\circ, \pm 45^\circ]$	4.656	26.374	84.984	5.532	31.377	101.232
	$[0^\circ, \pm 45^\circ, \pm 90^\circ]$	5.045	27.719	88.537	6.007	33.020	105.620
$a = 2l/3$	$[0^\circ, 0^\circ, \pm 30^\circ]$	4.167	22.996	78.161	4.959	27.345	93.051
	$[\pm 45^\circ, \pm 45^\circ]$	4.446	25.926	84.245	5.281	30.839	100.315
	$[0^\circ, \pm 45^\circ, \pm 90^\circ]$	4.809	27.221	87.813	5.724	32.420	104.722

the natural frequencies for the quasi-isotropic laminate are higher than the bending and torsion stiff laminates.

3.2 Analysis of Delamination Location Across the Thickness

In this section, the natural frequencies are evaluated for the square delamination at $a/l = 0.5$ (where a is a distance of delamination from the clamped end). The delamination location across the depth of plate is shown in Figure 7, In which t is the thickness of the plate and t' is the distance between the delamination point and top surface of the plate. The natural frequencies of E-glass and S-glass epoxy composite with different ply configurations are shown in Table 3 considering 33.33% of delamination. The results illustrate that the fundamental frequency decreases when delamination location changes from the top layer to mid-point.

3.3 Analysis of Percentage of Delamination

The effect of delamination size on the natural frequencies for both glass-epoxy composites is presented in this section. The square delaminations are considered at the mid-plane of the plate with different percentage of delamination as shown in Figure 8. Table 4 illustrates the influence of percentage (size) of delamination on the first three natural frequencies for different

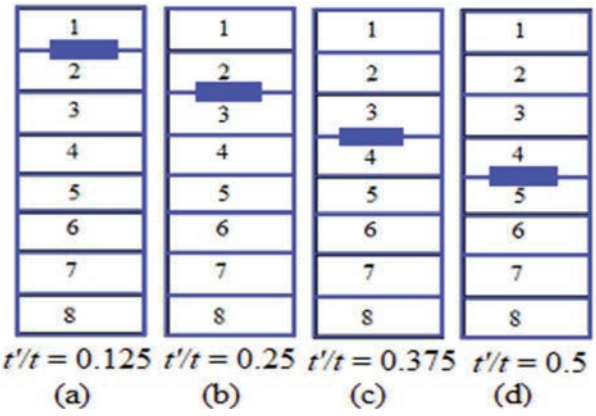

Figure 7 Delamination location across the thickness (t) of plate.

Table 3 Effects of delamination location across the thickness of the plate on the first three natural frequencies of *E*-glass and *S*-glass composite plates

Delamination Location	Fiber Orientation	Natural Frequencies (rad/s)					
		E-Glass			*S*-Glass		
		FNF	SNF	TNF	FNF	SNF	TNF
$t'/t = 0.125$	$[0°, 0°, \pm 30°]$	4.501	23.641	78.936	5.3617	28.124	93.871
	$[\pm 45°, \pm 45°]$	4.660	26.381	85.022	5.537	31.385	101.276
	$[0°, \pm 45°, \pm 90°]$	5.047	27.722	88.555	6.009	33.024	105.641
$t'/t = 0.25$	$[0°, 0°, \pm 30°]$	4.496	23.633	78.800	5.356	28.113	93.827
	$[\pm 45°, \pm 45°]$	4.656	26.374	84.991	5.532	31.377	101.240
	$[0°, \pm 45°, \pm 90°]$	5.045	27.717	88.532	6.007	33.018	105.613
$t'/t = 0.375$	$[0°, 0°, \pm 30°]$	4.495	23.628	78.782	5.354	28.108	93.804
	$[\pm 45°, \pm 45°]$	4.655	26.371	84.976	5.531	31.373	101.221
	$[0°, \pm 45°, \pm 90°]$	5.043	27.714	88.517	6.005	33.015	105.595
$t'/t = 0.5$	$[0°, 0°, \pm 30°]$	4.494	23.627	78.776	5.353	28.106	93.797
	$[\pm 45°, \pm 45°]$	4.654	26.369	84.970	5.530	31.371	101.214
	$[0°, \pm 45°, \pm 90°]$	5.043	27.713	88.513	6.004	33.013	105.590

ply configurations. The results show that the percentage of delamination is inversely proportional to all-natural frequencies irrespective of stacking sequence and composite materials. The natural frequency is minimum when delamination is 50%.

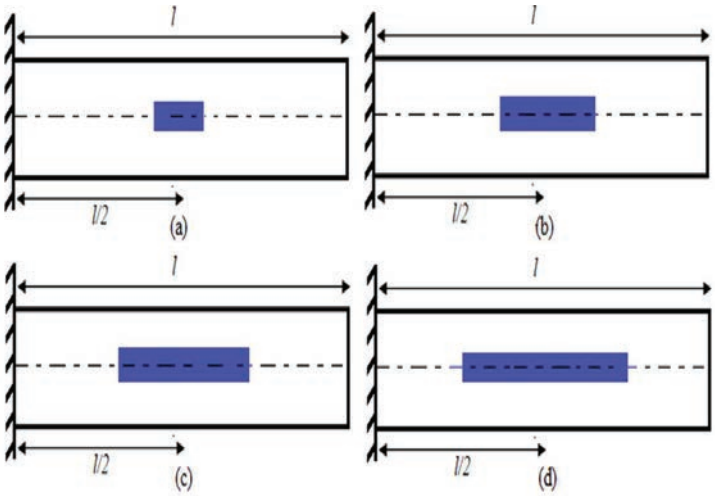

Figure 8 Different sizes of delamination [(a) 16.67% (b) 25% (c) 33.33% (d) 50%] at the mid-point of plate.

Table 4 Percentage of delamination at mid-point of the plate for different natural frequencies

% of Delamination	Fiber Orientation	Natural Frequencies (rad/s)					
		E-Glass			*S*-Glass		
		FNF	SNF	TNF	FNF	SNF	TNF
16.66%	$[0^\circ, 0^\circ, \pm 30^\circ]$	4.498	23.649	78.839	5.358	28.133	93.875
	$[\pm 45^\circ, \pm 45^\circ]$	4.656	26.376	84.993	5.532	31.380	101.24
	$[0^\circ, \pm 45^\circ, \pm 90^\circ]$	5.045	27.721	88.545	6.007	33.024	105.63
25%	$[0^\circ, 0^\circ, \pm 30^\circ]$	4.497	23.642	78.828	5.357	28.124	93.861
	$[\pm 45^\circ, \pm 45^\circ]$	4.655	26.374	84.984	5.532	31.377	101.230
	$[0^\circ, \pm 45^\circ, \pm 90^\circ]$	5.044	27.718	88.536	6.007	33.020	105.620
33.33%	$[0^\circ, 0^\circ, \pm 30^\circ]$	4.493	23.627	78.776	5.353	28.106	93.796
	$[\pm 45^\circ, \pm 45^\circ]$	4.654	26.369	84.969	5.530	31.371	101.210
	$[0^\circ, \pm 45^\circ, \pm 90^\circ]$	5.043	27.713	88.512	6.004	33.013	105.590
50%	$[0^\circ, 0^\circ, \pm 30^\circ]$	4.443	23.581	78.611	5.293	28.052	93.601
	$[\pm 45^\circ, \pm 45^\circ]$	4.614	26.291	84.729	5.530	31.371	101.210
	$[0^\circ, \pm 45^\circ, \pm 90^\circ]$	5.003	27.634	88.254	5.956	32.917	105.279

Table 5 Effect of ply orientation angle on the first three natural frequencies of *E*-glass and *S*-glass composite plate considering different numbers of delamination (N_d)

Ply Orientation angle			0°	15°	30°	45°	60°	75°	90°
E-Glass	$N_d = 0$	FNF	4.296	4.328	4.480	4.661	4.850	4.948	4.948
		SNF	21.560	22.637	24.730	26.388	27.373	27.588	27.314
		TNF	71.581	75.945	82.582	85.056	84.791	82.572	80.084
	$N_d = 1$	FNF	4.280	4.315	4.470	4.652	4.843	4.941	4.941
		SNF	21.528	22.609	24.720	26.369	27.347	27.562	27.288
		TNF	71.456	75.833	82.496	84.969	84.675	82.431	79.926
	$N_d = 4$	FNF	4.276	8.046	4.469	4.653	4.842	4.940	4.939
		SNF	21.518	39.078	24.715	26.364	27.340	27.555	27.281
		TNF	71.420	132.750	82.472	84.947	84.643	82.391	79.882
S-Glass	$N_d = 0$	FNF	5.122	5.155	5.329	5.539	5.759	5.874	5.874
		SNF	25.637	26.917	29.424	31.394	32.549	32.773	32.423
		TNF	85.067	90.362	98.375	101.318	100.925	98.170	95.108
	$N_d = 1$	FNF	5.103	5.138	5.316	5.529	5.751	5.866	5.865
		SNF	25.592	26.881	29.403	31.371	32.517	32.741	32.390
		TNF	84.914	90.225	98.270	101.214	100.785	98.001	94.919
	$N_d = 4$	FNF	5.097	5.135	5.314	5.528	5.750	5.864	5.863
		SNF	25.579	26.871	29.397	31.365	32.509	32.732	32.382
		TNF	84.870	90.185	98.241	101.187	100.747	97.953	94.866

3.4 Analysis of Ply-orientation Angle

In this section, effects of ply-orientation angle for the first three natural frequencies of laminated composite cantilever plates with zero, single and multiple delamination are determined as shown in Table 5. The natural frequencies are directly proportional to ply-orientation angle for un-delamination as well as for single and multi-delamination. The results present the natural frequencies of *E*-Glass and *S*-Glass epoxy laminated composite and found the reduction in global stiffness of *S*-Glass is lower than the *E*-Glass with the increase in ply-orientation angle. The mode shapes (obtained by ANSYS) for first three natural frequencies for different ply angles of an un-delaminated E-glass and S-glass epoxy composite cantilever plate are presented in Figures 9 and 10.

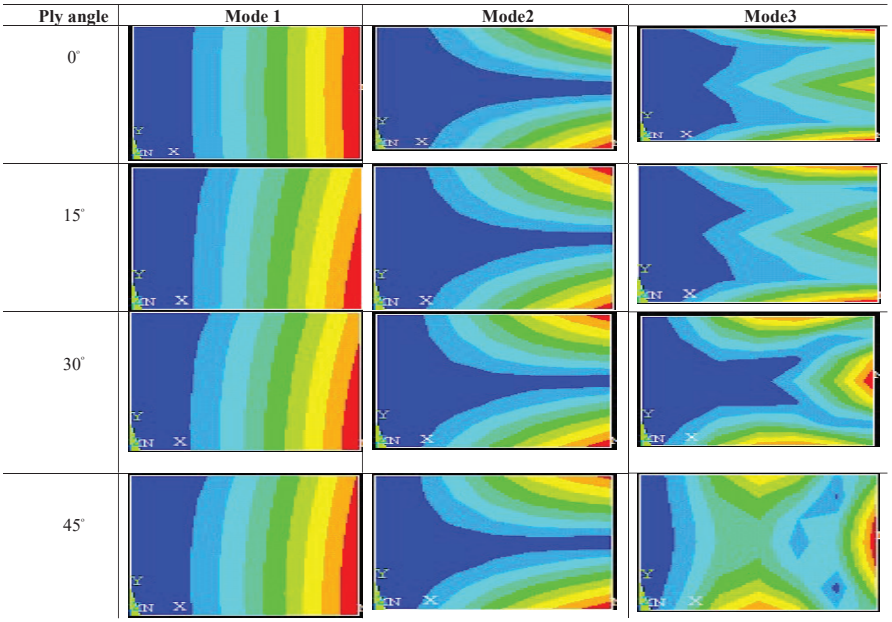

Figure 9 Mode shapes of *S*-Glass for different ply angle with no delamination.

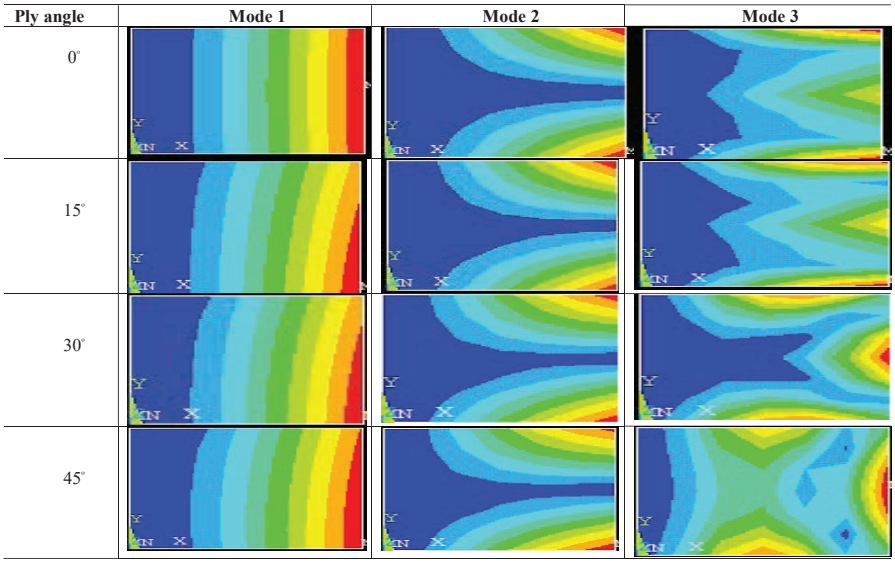

Figure 10 Mode shapes of *E*-Glass for different ply angle with no delamination.

4 Conclusions

In this paper, the effect of location, size of delamination and plate geometry viz. ply-orientation angle are investigated for the natural frequencies of a cantilever composite plate. FEM is employed for free vibration analysis of single and multiple delamination E-glass epoxy and S-glass epoxy composite plate. The result illustrates that the delamination in plate decreases global stiffness and performance of the composite structures. The natural frequencies are observed to be varying with change in location and size of the delamination. The natural frequencies are also observed to be varying with change in ply-orientation angle and have the maximum value for 45° and 90° with respect to no delamination case. A comparative study is carried out between the natural frequencies of *E*-glass and *S*-glass epoxy composite considering different types of laminates. In future, further study can be conducted by some advanced method such as adaptive meshing on complex structures.

References

[1] Della C.N. and D. Shu "Vibration of delaminated composite laminates: A review" *Applied Mechanics Reviews*, 60/1 1–20, 2017

[2] Nanda N. and S.K. Sahu "Free vibration analysis of delaminated composite shells using different shell theories" *International Journal of Pressure Vessels and Piping*, 98, 111–118, 2012.

[3] Campanelli R.W. and J.J. Engblom "The effect of aminations in graphite/PEEK composite plates on modal dynamic characteristics" *Composite structures*, 31/3, 195–202. *Composites Letters*, 25/2, 43–48, 1995.

[4] Fu, F., "3D finite element analysis of the whole-building behavior of tall building in fire". Advances in Computational Design, 1(4), pp. 329–344, 2016.

[5] Hu, N., H. Fukunaga, M. Kameyama, Y. Aramaki and F.K. Chang "Vibration analysis of delaminated composite beams and plates using a higher-order finite element" *International Journal of Mechanical Sciences*, 44/7, 1479–1503, 2002.

[6] Polatov, A.M., Khaldjigitov, A.A. and Ikramov, A.M., "Algorithm of solving the problem of small elastoplastic deformation of fiber composites by FEM". Advances in Computational Design, 5(3), pp. 305–321, 2020.

[7] Krawczuk M. and W.M. Ostachowicz, "Modelling and vibration analysis of a cantilever composite beam with a transverse open crack" *Journal of Sound and Vibration*, 183/1, 69–89, 1995.
[8] Kaya A.I., M. Kisa, M. Ozen, "Influence of natural weathering conditions on the natural frequency change of woven carbonfibre reinforced composites" *Advanced Composites Letters*, 27/ 2, 49–54, 2018.
[9] Dey S., T. Mukhopadhyay, A. Spickenheuer, U. Gohs and S. Adhikari, "Uncertainty quantification in natural frequency of composite plates-An Artificial neural network based approach" *Advanced Composites Letters*, 25/2, 43–48, 2016.
[10] Birman V. and L.W. Byrd, "Effect of matrix cracking in cross-ply ceramic matrix composite beams on their mechanical properties and natural frequencies" *International journal of non-linear mechanics*, 38/2, 201–212, 2003.
[11] Ramkumar R.L., S.V. Kulkarni, R.B. Pipes, "Free vibration frequencies of a delaminated beam" *Reinforcing the future*, 1979.
[12] Wang J.T.S., Y.Y. Liu, J.A. Gibby, "Vibrations of split beams" *Journal of Sound and Vibration*, 84/4, 491–502, 1982.
[13] Kalita K., M. Ramachandran, P. Raichurkar, S.D. Mokal and S. Haldar, "Free vibration analysis of laminated composites by a nine node isoparametric plate bending element" *Advanced Composites Letters*, 25/5, 108–116, 2016.
[14] Ercopur T. and B.G. Kiral, "Investigation of free vibration response of E-glass/epoxy delaminated composite plates" *Advanced Composites Letters*, 21/1, 5–15, 2012.
[15] Saravanos D.A. and D.A. Hopkins, "Effects of delaminations on the damped dynamic characteristics of composite laminates: analysis and experiments" *Journal of Sound and Vibration*, 192/5, 977–993, 1996.
[16] Kisa M., "Free vibration analysis of a cantilever composite beam with multiple cracks" *Composites Science and Technology*, 64/9, 1391–1402, 2004.
[17] Perel V.Y., "Finite element analysis of vibration of delaminated composite beam with an account of contact of the delamination crack faces, based on the first-order shear deformation theory" *J. of compo. material*, 39/20, 1843–1876, 2005.
[18] Viola E., M. Dilena and F. Tornabene, "Analytical and numerical results for vibration analysis of multi-stepped and multi-damaged circular arches" *J. of So. And Vibra.*, 299/1–2, 143–163, 2007.

[19] Qatu M. S., A.W. Leissa, "Vibration studies for laminated composite twisted cantilever plates" *International Journal of Mechanical Sciences*, 33/11, 927–940, 1991.

[20] Karsh, P. K., R. R. Kumar, and S. Dey. "Radial basis function-based stochastic natural frequencies analysis of functionally graded plates." *International Journal of Computational Methods* 17, 09, 2020: 1950061.

[21] Karsh, P. K., T. Mukhopadhyay, and S. Dey. "Stochastic investigation of natural frequency for functionally graded plates." *In IOP conference series: materials science and engineering*, 326, 1, p. 012003. IOP Publishing, 2018.

[22] Karsh, P. K., H. P. Raturi, R. R. Kumar, and S. Dey. "Parametric uncertainty quantification in natural frequency of sandwich plates using polynomial neural network." *In IOP Conference Series: Materials Science and Engineering*, 798, 1, p. 012036. IOP Publishing, 2020.

[23] Karsh P.K., T. Mukhopadhyay and S. Dey, "Stochastic dynamic analysis of twisted functionally graded plates" *Composites Part B: Engineering*, 147, 259–278, 2018.

[24] Shen M.H. and J.E. Grady, Free vibrations of delaminated beams. *AIAA Journal*, 30/5, 1361–1370, 1992.

[25] Dey S. and A. Karmakar, "Effect of Multiple Delamination on Free Vibration Behaviour of Quasi-Isotropic Composite Conical Shells" *Journal of The Inst. of Engineers: Series C*, 94/1, 53–63, 2013.

[26] Dey S. and A. Karmakar, "Effect of location of delamination on free vibration of cross-ply conical shells". *Shock and Vibration*, 19/4, 679–692, 2012.

[27] R.M. Jones, "Mechanics of Composite Materials" (Hemisphere, New York), 147–156, 1975

[28] Ercopur, Turan, and Binnur Goren Kiral. "Investigation of free vibration response of E-glass/epoxy delaminated composite plates." Advanced Composites Letters 21 (1), 2012: 096369351202100101.

Biographies

P. K. Karsh received the bachelor's degree in Industrial and Production Engineering from Guru Ghasdas Central University, Bilaspur, India in 2012, the master's degree in Industrial and Production Engineering from National Institute of Technology, Kurukshetra, India in 2016, and the philosophy of doctorate degree in Mechanical Engineering from National Institute of Technology Silchar, India in 2019, respectively. He is currently working as an Assistant Professor at the Department of Mechanical Engineering, Faculty of Engineering & Technology, Parul University, India. His research areas include, stochastic free vibration analysis, impact analysis and failure analysis of composite and functionally graded materials. He has been serving as a reviewer for many highly-respected journals.

Bindi Thakkar received the bachelor's degree in Industrial and Mechanical Engineering from D. Y. Patil College of Engineering Pune, India in 2006, the master's degree in CAD/CAM from Bharti Vidhyapeeth University, Pine India in 2009, and pursuing PhD in Design and Manufacturing from Parul University in 2020 respectively. She is currently working as an Head Of

the Department and Assistant Professor at the Department of Mechanical Engineering, Faculty of Engineering & Technology, Diploma Studies, Parul University, India. She has 14 years of teaching experience at Parul University, since 2008. Her research areas include, Composites, stochastic free vibration analysis, impact analysis and failure analysis of composite and functionally graded materials.

R. R. Kumar received the bachelor's degree in Mechanical Engineering from Rajasthan Technical University, Kota, India in 2014, the master's degree in Mechanical Engineering from Natioal Institute of Technology, Silchar, India in 2016, and the doctor of Philosophy degree in Mehcnaical Engineering from Natioal Institute of Technology Silchar, India in 2019, respectively. His research area includes: composite structure, stochastic analysis, surrogate modelling, impact analysis, vibration analysis and computational mechanics. He has been serving as a reviewer for several international journals.

Abhijeet kumar has obtained his Bachelor's degree in Mechanical Engineering from Hindustan College of science and technology, Uttar pradesh, India in 2014, The master's degree in CAD/CAM & Automation from

National Institute of technology, silchar, India in 2018. He has also worked as project intern in Industrial Engineering Department at IIT, Kharagpur, India. He is currently working as a junior manager, Automation & Robotics at Tatametaliks Ltd, India. His research interests include Automation, Robotics, digitalization, impact and failure analysis of composite and functionally graded materials.

Sudip Dey is a faculty in the Mechanical Engineering Department of National Institute of Technology Silchar, India. Previously, He was a Post-doctoral Researcher at Leibniz-Institut für Polymerforschung Dresden e. V., Germany, worked with Prof. Gert Heinrich (TU Dresden, Germany). Prior to that he was a Post-doctoral Researcher at College of Engineering, Swansea University, United Kingdom, worked with Prof. Sondipon Adhikari. He obtained Bachelor in Mechanical Engineering Degree from Jadavpur University, India. He received Ph.D. (Engg.) degree from Jadavpur University, India. His field of specialization is Applied Mechanics and Design. He has more than fifteen years of experience in research, teaching, industrial and professional activities. He is actively engaged in academics, teaching, research and industrial projects. His research interests include molecular dynamics, multi-scale and computational investigation of fibre-matrix interaction, uncertainty quantification, mechanics of composite and functionally graded structures, finite element analyses, digital twin with an emphasis on computational modelling.